AFRL-ML-WP-TP-2007-517

ABSORPTION OF NARROW GAP HgCdTe NEAR THE BAND EDGE INCLUDING NONPARABOLICITY AND THE URBACH TAIL (PREPRINT)

Yong Chang, Christoph H. Grein, S. Sivananthan, Shekhar Guha, S. Velicu, M.E. Flatté, and V. Nathan

Hardened Materials Branch
Survivability and Sensor Materials Division

JANUARY 2007

AIR FORCE RESEARCH LABORATORY
MATERIALS AND MANUFACTURING DIRECTORATE
WRIGHT-PATTERSON AIR FORCE BASE, OH 45433-7750
AIR FORCE MATERIEL COMMAND
UNITED STATES AIR FORCE

NOTICE AND SIGNATURE PAGE

AFRL-ML-WP-TP-2007-517 HAS BEEN REVIEWED AND IS APPROVED FOR PUBLICATION IN ACCORDANCE WITH ASSIGNED DISTRIBUTION STATEMENT.

*//Signature//

SHEKHAR GUHA, Ph.D.
Agile IR Limiters
Exploratory Development
Hardened Materials Branch

//Signature//

MARK S. FORTE, Acting Chief
Hardened Materials Branch
Survivability and Sensor Materials Division

//Signature//

TIM J. SCHUMACHER, Chief
Survivability and Sensor Materials Division

*Disseminated copies will show "//Signature//" stamped or typed above the signature blocks.

REPORT DOCUMENTATION PAGE

Form Approved
OMB No. 0704-0188

1. REPORT DATE *(DD-MM-YY)*	2. REPORT TYPE	3. DATES COVERED *(From - To)*
January 2007	Journal Article Preprint	

4. TITLE AND SUBTITLE

ABSORPTION OF NARROW GAP HgCdTe NEAR THE BAND EDGE INCLUDING NONPARABOLICITY AND THE URBACH TAIL (PREPRINT)

5a. CONTRACT NUMBER
In-house

5b. GRANT NUMBER

5c. PROGRAM ELEMENT NUMBER
62102F

6. AUTHOR(S)

Yong Chang, Christoph H. Grein, and S. Sivananthan (University of Illinois at Chicago)
Shekhar Guha (AFRL/MLPJ)
S. Velicu (EPIR Technologies, Inc.)
M.E. Flatté (University of Iowa)
V. Nathan (Air Force Research Laboratory, Kirtland AFB)

5d. PROJECT NUMBER
4348

5e. TASK NUMBER
RG

5f. WORK UNIT NUMBER
M08R1000

7. PERFORMING ORGANIZATION NAME(S) AND ADDRESS(ES)

University of Illinois at Chicago
Department of Physics (MC273)
Chicago, IL 60607

Hardened Materials Branch (AFRL/MLPJ)
Survivability and Sensor Materials Division
Materials and Manufacturing Directorate
Wright-Patterson Air Force Base, OH 45433-7750
Air Force Materiel Command, United States Air Force

EPIR Technologies, Inc.
Bolingbrook, IL 60440

University of Iowa
Department of Physics and Astronomy
Iowa City, IA 52242

Air Force Research Laboratory
3550 Aberdeen Ave. SE
Kirtland AFB, NM 87117

8. PERFORMING ORGANIZATION REPORT NUMBER
AFRL-ML-WP-TP-2007-517

9. SPONSORING/MONITORING AGENCY NAME(S) AND ADDRESS(ES)

Air Force Research Laboratory
Materials and Manufacturing Directorate
Wright-Patterson Air Force Base, OH 45433-7750
Air Force Materiel Command
United States Air Force

10. SPONSORING/MONITORING AGENCY ACRONYM(S)
AFRL/MLPJ

11. SPONSORING/MONITORING AGENCY REPORT NUMBER(S)
AFRL-ML-WP-TP-2007-517

12. DISTRIBUTION/AVAILABILITY STATEMENT
Approved for public release; distribution unlimited.

13. SUPPLEMENTARY NOTES
Journal article submitted to the Journal of Electronic Materials.

The U.S. Government is joint author of this work and has the right to use, modify, reproduce, release, perform, display, or disclose the work.

PAO Case Number: AFRL/WS 06-2742, 27 Nov 2006.

14. ABSTRACT

An analytical model describing the absorption behavior of Hg1-xCdxTe is developed. It simultaneously considers the contributions from non-parabolic conduction/light hole bands and parabolic heavy hole bands obtained from 14-band k˙p electronic structure calculations as well as the Urbach tail. This model smoothly fits experimental absorption coefficients over energies ranging from the Urbach tail region to the intrinsic absorption region up to at least 300 me V above the band gap.

15. SUBJECT TERMS
HgCdTe, Absorption, Absorption coefficient, Band structure, Optical constant, Infrared

16. SECURITY CLASSIFICATION OF:			17. LIMITATION OF ABSTRACT:	18. NUMBER OF PAGES	19a. NAME OF RESPONSIBLE PERSON (Monitor)
a. REPORT	b. ABSTRACT	c. THIS PAGE			Shekhar Guha
Unclassified	Unclassified	Unclassified	SAR	28	19b. TELEPHONE NUMBER *(Include Area Code)* N/A

Standard Form 298 (Rev. 8-98)
Prescribed by ANSI Std. Z39-18

Absorption of Narrow Gap HgCdTe Near the Band Edge Including Nonparabolicity and the Urbach Tail

Yong Chang[a)*], S. Guha[b)], Christoph H. Grein[a)], S. Velicu[c)], M.E. Flatté[d)], V. Nathan[e)], and S. Sivananthan[a)]

a) *Microphysics Laboratory, Department of Physics (MC273), University of Illinois at Chicago, Chicago, IL 60607*

b) *Air Force Research Laboratories, Wright Patterson AFB, OH 45433*

c) *EPIR Technologies Inc., Bolingbrook, Illinois 60440*

d) *Department of Physics and Astronomy, University of Iowa, Iowa City, IA 52242*

e) *Air Force Research Laboratory, Kirtland AFB, NM 87117*

Abstract

An analytical model describing the absorption behavior of $Hg_{1-x}Cd_xTe$ is developed. It simultaneously considers the contributions from non-parabolic conduction/light hole bands and parabolic heavy hole bands obtained from 14-band k·p electronic structure calculations as well as the Urbach tail. This model smoothly fits experimental absorption coefficients over energies ranging from the Urbach tail region to the intrinsic absorption region up to at least 300 meV above the band gap.

Key words: HgCdTe, Absorption, Absorption coefficient, Band structure, Optical constant, Infrared

PACS: 78.20.Bh, 78.30.Fs, 71.28.+d and 71.20.Nr

Introduction

The narrow gap semiconductor alloy $Hg_{1-x}Cd_xTe$ is the dominant material for the fabrication of high performance infrared photon detectors and detector arrays. The absorption coefficient is one of the most important factors that determines the quantum efficiency of an infrared detector element. The absorption coefficient as a function of absorbed photon energy in the vicinity of the optical energy gap E_0 has two major regions: 1) below E_0 follows Urbach's rule describing transitions between localized band-tail states, and 2) above E_0 to approximately 300 meV over E_0 (hence far below the next critical point in the absorption structure), called the intrinsic or Kane region, describing transitions between extended valance and conduction band states. From the theoretical perspective, that precise measurements and analytical models of absorption coefficients as functions of absorbed photon energies, as described in this paper, shed light on the actual band structure of HgCdTe, which is extremely important for the study of the material properties of HgCdTe, e.g. effective masses, and radiative and Auger carrier recombination lifetimes. From the applications perspective, modern HgCdTe detectors with advanced architectures usually employ devices with thin absorber layers, so the cut-off wavelength is determined by photons with high absorption coefficients (up to 10^4 cm^{-1}) because the 50% cut-off of a idea detector is determined by both the absorption coefficient and absorber layer thickness. Figure 1 shows the calculated 50% cut-off as a function of absorber layer thickness. As the thickness decreases, the cut-off is established with higher absorption coefficients and hence shorter wavelengths. For examples, the 50% cut-off wavelength of a detector with a 1 μm thick absorber layer at 77 K is about 5 μm, which corresponds to $Hg_{0.69}Cd_{0.31}Te$ according to Hansen-Schmit-Casselman's formula.[1] Therefore, knowledge of the dependence of the absorption coefficient on photon energy in the intrinsic region is critical to precisely determine the cut-off of detectors employing thin HgCdTe absorber layers. Our model exhibits good agreement

with experimental data in this region, whereas previous models [2, 3] using parabolic band approximations show significant deviations.

Experimental

HgCdTe samples were grown on CdZnTe (211)B substrates in a Riber 32P molecule beam epitaxy (MBE) system equipped with *in situ* spectroscopic ellipsometry (SE) that is sensitive from the near infrared to the ultraviolet spectral bands. SE improves material uniformity and MBE growth controllability, and hence yields better material quality and yield.[4] The high material quality, high composition and thickness uniformity both along[5] and perpendicular[6] to the growth direction, and the good optical flatness of HgCdTe epilayers enable reliable measurement of the absorption coefficient over the 10^2 to 10^4 cm^{-1} range, which covers both the Urbach tail and intrinsic absorption (up to 300 meV) regions. The details of the growth procedure, quality control and growth conditions optimization are discussed elsewhere.[7,8,9] The samples are n-type (intentionally doped with In with a doping level in the low $10^{15}cm^{-3}$ range), with visible surface defects such as craters[10,11], voids and microtwins less than mid-10^3 cm^{-2} in density and threading dislocation densities in the low 10^5 cm^{-2} as revealed by etch pit density measurements using Schaake's etchant[12]. They are selected to be representative of standard n-type absorber regions of typical photodiodes.

The infrared transmission measurements were performed on a Thermo Nicolet 870 research class Fourier transform infrared spectrometer with an Oxford CF1204 static exchange continuous flow liquid helium cryostat. The spectral range of infrared transmission measurements with this experimental set-up is from the visible to 200 μm. The samples were mounted on the cold finger of a cryostat in a helium atmosphere. Thermal exchanges occur primarily through the surrounding helium atmosphere to ensure a homogeneous temperature distribution in the HgCdTe samples over a temperature range from about 4 K to room temperature. In order to obtain a maximum precision for

the determination of cut-offs, the transmissivity and photoconductivity were simultaneously measured at the same points on the samples. We used the interference matrix method[13] (also called the thin film transmission matrix method by some other researchers[14]) to calculate the sample thickness[6] and then calculated the absorption coefficient from the measured transmissivity data.[15]

Note that long wavelength infrared (8-12 μm cutoff wavelength) HgCdTe with Cd compositions from 0.21 to 0.23 and operating temperatures of about 77 K are the focus of this work. Long wavelength infrared is an overwhelming application field of HgCdTe and 77 K is of primary importance because most of HgCdTe detectors (as well as other high performance infrared detectors) require liquid nitrogen operating temperatures. We do not discuss wider bandgap HgCdTe in this paper because the parabolic model has been shown to be excellent for wide bandgap semiconductors. Burstein-Moss shifts due to band filling effects is not taken into account in this work; they are anticipated to influence the shape of the absorption coefficient curve at high temperatures or at low temperatures in heavily doped samples.

Results and Discussions

Previous works[3, 15, 16, 17] have demonstrated that the absorption coefficient of HgCdTe below energy gap E_g can be fitted by the formula suggested by Urbach[18] as follows: [19]

$$\alpha = \exp[(\hbar\omega - E_0)/W] = \alpha_0 \exp(\hbar\omega/W) \qquad (\hbar\omega < E_0) \tag{1}$$

where $\hbar\omega$ is the absorbed photon energy, E_0 is a reference energy, specifically, we assign it the value of optical band gap, α_0 is the absorption coefficient at the energy of E_0, and W is the Urbach slope in the same units as $\hbar\omega$ describing the steepness of the Urbach absorption tail. The Urbach absorption tail energy as a function of temperature has been discussed elsewhere in detail.[15] Its magnitude measures the combined contribution from static and dynamic disorders. The contribution of static

disorder, including structural and alloy disorder, was found to dominate the Urbach energy of HgCdTe at low temperatures. Alloy disorder is mainly a function of alloy composition in $Hg_{1-x}Cd_xTe$, whereas structural disorder is determined by substrate and buffer layer species and quality, growth conditions, thermal processing history, crystalline perfection and doping. The structural disorder may vary from sample to sample and also from area to area within the same sample, as revealed by infrared microscope mapping.[4,20]

The Kane model,[21] based on the 8×8 matrix $k \cdot p$ approach, is the most commonly employed model to describe the band structure near the Γ point of narrow gap semiconductors with non-parabolic bands. The dispersion relationships of the conduction band [$E_c(k)$], the heavy hole band [$E_{hh}(k)$] and the light hole band [$E_{lh}(k)$] are given by the analytical formulas:

$$\begin{cases} E_c = \dfrac{\hbar^2 k^2}{2m_0} + \dfrac{1}{2}\left(Eg + \sqrt{Eg^2 + \dfrac{8}{3}k^2P^2} \right) \\ E_{hh} = -\dfrac{\hbar^2 k^2}{2m_{hh}} \\ E_{lh} = \dfrac{\hbar^2 k^2}{2m_0} + \dfrac{1}{2}\left(Eg - \sqrt{Eg^2 + \dfrac{8}{3}k^2P^2} \right) \end{cases} \tag{2}$$

where E_c, E_{hh} and E_{lh} are the conduction band, heavy hole band and light band energies measured from the top of the valance band, respectively, k is the electron crystal momentum, m_0 is the free electron mass, E_g is the energy band gap, P is the momentum matrix element with a value of 8.0 to 8.5 $\times 10^{-8}$ eV·cm[22,23], and m_{hh}^* is the heavy hole effective mass with a value of about $0.5m_0$ for HgCdTe. The spin orbit splitting energy of HgCdTe varies from 0.96 to 1 eV, which is out of the energy range considered in this paper and is hence neglected. Since the contributions to both E_c and E_{lh} from the first term $\frac{\hbar^2 k^2}{2m_0}$ are less than 1% up to 200 meV beyond the band edge and therefore negligible, E_c can be written in the hyperbolic form:

$$E_C = \sqrt{s^2k^2 + b^2} - b + E_g \tag{3}$$

where b=E_g/2 and $s = \pm\sqrt{2P^2/3}$ are the slopes of the two asymptotes. This formula describes a hyperbola with origin at (0, E_g/2) in the E-k plane, semimajor axis b parallel to the y-axis and semiminor axis parallel to the x-axis. The eccentricity of the curve is $\sqrt{1+s^2}$. A similar result can also be obtained for the light hole band, which is a symmetric hyperbola of E_c-k in the energy range of 400 meV below the top of the valance band.

More precise $k \cdot p$ calculations using a 14×14 matrix give similar hyperbolae describing the E_c or E_{lh} dispersions. Figures 2(a) to (d) show 14×14 $k \cdot p$ calculated band structure results for $Hg_{0.77}Cd_{0.23}Te$ at the temperatures of 300 K, 200 K, 100 K and 77 K, respectively; Figs 2(e) and (f) show fittings to Eq.(3) for $Hg_{0.77}Cd_{0.23}Te$ at a temperature of 77 K. As shown in Fig. 2, the band structure maintaions the same E-k dispersion relationship at all temperatures, which includes the hyperbolic conduction bands and light hole bands (down to 400 meV below the top of valance bands), as well as the parabolic heavy hole bands. As already mentioned, the spin-splitting bands are out of the energy range considered in this paper due to the spin orbit splitting energy of HgCdTe being 0.96 to 1 eV, and are hence neglected. In addition, as shown in Fig. 2, the fits require that both s and b no longer take the values implied by Eq. 2., i.e. b=E_g/2 and $s = \pm\sqrt{2P^2/3}$, hence s and b can only be determined by fitting the calculated energy band structures, namely they act as two parameters describing the shape of both conduction and light hole bands (because these two bands are symmetric with one another). Specifically, E_c fits give s = 8850.01 ± 10.20 (× 10^{-11}eV·cm) and b=103.354 ± 2.035 (meV). Similar results for HgCdTe with a similar composition at 0 K were also obtained by Krishnamurthy *et al.* [24] using a hybid pseudopotential tight-binding method for calculating the electronic band structure. The asymptotes can be used to approximate the E_c dispersion

relationship when E or k is large. According to Fig. 2, near the energy of 150 meV above the bottom of the conduction band, the dispersion relationship becomes linear. On the other hand, when k is small, the lowest order term of a Taylor series of Eq. 3 will give a reasonable approximation:

$$E_C = E_g + \frac{s^2}{2b}k^2 \tag{4}$$

which describes a parabolic E_c dispersion relationship near the Γ point, as shown in Fig. 2(f). The electron effective mass is obtained from $m_e^* / m_0 = \frac{\hbar^2 b}{s^2 m_0}$

Noting that the optical matrix elements vary slowly with k, and restricting our attention to energies near the band gap (-20 meV $\leq \hbar\omega - E_g \leq$ 400 meV), we discuss the absorption behavior assuming that the optical matrix elements can be treated as constant. The absorption coefficient of HgCdTe is then given by:

$$\alpha = \frac{A}{\hbar\omega} \cdot \rho_{CV}(k) \tag{5a}$$

where $$\rho_{CV}(k) = \int \frac{2}{(2\pi)^3} d^3k \cdot \delta[E_c(k) - E_v(k) - \hbar\omega] \tag{5b}$$

A is a constant, $\hbar\omega$ is the energy of absorbed photons, and ρ_{CV} is the joint density of states. Considering spherical iso-energy surfaces and employing the properties of Dirac's δ function, ρ_{CV} can be rewritten as:

$$\rho_{CV}(k) = \int_{E_c(k)-E_v(k)=\hbar\omega} \frac{ds}{\nabla_k (E_C(k) - E_V(k))} \cdot \frac{1}{4\pi^3} = \frac{K^2}{\pi^2} \left(\frac{\partial E_C}{\partial K} - \frac{\partial E_j}{\partial K}\right)^{-1} \Bigg|_{E_c(K)-E_j(K)=\hbar\omega} \tag{6}$$

where K_j are the values of one dimension electron crystal momentum that fit the conditions $E_C(K_j)$-$E_j(K_j)$=ħω, j represents the light or heavy hole bands. Therefore, the total absorption coefficient α,

which is the sum of absorption coefficient involving light hole (α_{lh}) and heavy hole (α_{hh}) bands, can be given as a function of ħω or $\varepsilon = \hbar\omega - E_g$:

$$\alpha_{hh} = \frac{A}{\pi^2(\varepsilon + E_g)} \cdot K_{c-hh} \cdot \left[\frac{s^2}{\sqrt{s^2 K_{c-hh}^2 + b^2}} + \frac{\hbar^2}{m_{hh}^*} \right]^{-1} \tag{7a}$$

K_{c-hh} as a function of ε can be obtained by solving the following equation:

$$\varepsilon = \sqrt{s^2 K_{c-hh}^2 + b^2} - b + \frac{\hbar^2}{2m_{hh}^*} K_{c-hh}^2 \tag{7b}$$

Let $\varepsilon_c = \sqrt{s^2 K_{c-hh}^2 + b^2} - b$ and $\varepsilon_{hh} = (\hbar^2 / 2m_{hh}^*) K_{c-hh}^2$, then $\varepsilon_c + \varepsilon_{hh} = \varepsilon$ and ε_c, ε_{hh} correspond to the same electron crystal momentum K_{c-hh}^2. Because of the significant difference between the electron and hole effective masses, it's a good approximation to set $\varepsilon = \varepsilon_c$. Then Eq. 7(a) can be rewritten as:

$$\alpha_{hh} = \frac{A}{\pi^2 s^3 (\varepsilon + E_g)} (\varepsilon + b) \sqrt{(\varepsilon + b)^2 - b^2} \tag{8}$$

Because the conduction and light hole bands are symmetrical in the energy range of 400 meV beyond the band gap, we get:

$$\alpha_{lh} = \frac{A}{\pi^2(\varepsilon + E_g)} \left[\frac{1}{2} \cdot \frac{1}{s^3} \left(\frac{\varepsilon}{2} + b\right) \sqrt{\left(\frac{\varepsilon}{2} + b\right)^2 - b^2} \right] = \frac{A}{\pi^2 s^3 (\varepsilon + E_g)} \left[\frac{1}{8} (\varepsilon + 2b) \sqrt{(\varepsilon + 2b)^2 - (2b)^2} \right] \tag{9}$$

Therefore, the total absorption coefficient above the energy gap E_g as a function of absorbed photon energy $\hbar\omega$ is:

$$\begin{aligned} \alpha = \alpha_{hh} + \alpha_{lh} &= \frac{A}{\pi^2 s^3 (\varepsilon + E_g)} \left[(\varepsilon + b) \sqrt{(\varepsilon + b)^2 - b^2} + \frac{1}{8} (\varepsilon + 2b) \sqrt{(\varepsilon + 2b)^2 - (2b)^2} \right] \\ &= \frac{B}{\hbar\omega} \left[(\hbar\omega - E_g + b) \sqrt{(\hbar\omega - E_g + b)^2 - b^2} + \frac{1}{8} (\hbar\omega - E_g + 2b) \sqrt{(\hbar\omega - E_g + 2b)^2 - (2b)^2} \right] \end{aligned} \tag{10}$$

Note that $B = A\pi^{-2} s^{-3}$ is a constant.

Eq. 10 was used to fit the experimentally measured absorption coefficient of a $Hg_{0.79}Cd_{0.21}Te$ sample at 80 K; the results are shown in Fig.3. When the photon energy is much larger than the absorption edge, i.e. $\varepsilon = \hbar\omega - E_g$ is very large, the conditions $\varepsilon + 2b >> 2b$ and $\varepsilon + b >> b$ will be met, and Eq. 10 can be rewritten as:

$$\alpha = \frac{A}{\pi^2(\varepsilon + E_g)} \cdot \frac{1}{s^3} \cdot \frac{1}{8}\left[8(\varepsilon + b)^2 + (\varepsilon + 2b)^2\right] = \frac{C(\hbar\omega - E_g + D)^2 + F}{\hbar\omega} \tag{11}$$

where $C = \frac{9A}{8s^3\pi^2}$, $D = \frac{10}{9}b$ and $F = \frac{A}{9s^3\pi^2}b^2$. Note that the product of the absorption coefficient and the energy $(\alpha\hbar\omega)$ varies as the square of the energy when the energy is greater than E_g by hundreds of meV. Equation 11 can also be obtained if one substitutes the $E_C(k)$ and $E_{lh}(k)$ relations by the asymptote of Eq. 3.

Within about 20 meV of the energy gap, $\varepsilon = \hbar\omega - Eg << b$. Equation 10 can then be rewritten as:

$$\begin{aligned} \alpha &= \frac{A}{\pi^2 s^3(\varepsilon + E_g)}\left[(\varepsilon + b)\sqrt{\varepsilon}\cdot\sqrt{\varepsilon + 2b} + \frac{1}{8}(\varepsilon + 2b)\sqrt{\varepsilon}\sqrt{\varepsilon + 4b}\right] \\ &= \frac{A}{\pi^2 s^3(\varepsilon + E_g)}\left[b\sqrt{\varepsilon}\cdot\sqrt{2b} + \frac{1}{8}(2b)\sqrt{\varepsilon}\sqrt{4b}\right] = \frac{Ab^{\frac{3}{2}}}{\pi^2 s^3(\hbar\omega)}\left[\sqrt{2} + \frac{1}{2}\right]\cdot\sqrt{\hbar\omega - E_g} \end{aligned} \tag{12}$$

In fact, when ε or k is small, Eq. 3 can be used as an approximation of $E_c(k)$ and $E_{lh}(k)$, and Eq. 12 can be derived as well. An example is shown in Fig. 3. An empirical formula with a similar form has been suggested by Schacham et al. [25] from absorption very near the band gap in samples with thicknesses of 25 μm to 300 μm.[3]

Eqs. 10, 11 and 12 give a clear picture of the changing tendency of $\alpha\cdot\hbar\omega$ with ħω, which can be combined into the formula $\alpha\cdot\hbar\omega \propto \varepsilon^{f(\varepsilon)}$, where $f(\varepsilon)$ is a function of ε taking the values of 0.5 to 2. $f(\varepsilon) = 0.5$ when ε is very small. With increasing ε, $f(\varepsilon)$ gradually increases. When ε is very large, $f(\varepsilon)$ takes the value of 2. Therefore, depending on the range of energy above the band gap, an

empirical formula of $\alpha \cdot \hbar\omega \propto \varepsilon^{\gamma}$ $(0.5 \le \gamma \le 2)$ can be used to describe the energy dependence of the absorption coefficient near the band gap, where $\gamma = \frac{1}{n}\sum_{n} f(\varepsilon_i)$, i.e. an average over n energy points taken into account during the fitting calculations above E_g. Such a result can also be derived from Eq. 6 through assuming the dispersion relationships $E_C(k) = k^{\frac{3}{1+\gamma}} + E_g$ and $E_{lh}(k) = -k^{\frac{3}{1+\gamma}}$. As shown in Fig. 2(c), such assumptions are reasonably correct as long as $1 \le \frac{3}{1+\gamma} \le 2$, corresponding to $0.5 \le \gamma \le 2$, being exactly the same range as in our previous discussions. Moazzami et al. [26] have empirically determined a γ value of about 0.7 for a $Hg_{0.69}Cd_{0.31}Te$ sample in the energy range of about 100 meV above the energy gap. Chu and co-workers [17,27] found that a logarithmic approximation works best in the energy range of 100 meV above the energy gap.

The absorption coefficient below the energy gap is expected to follow the Urbach rule. To guarantee a smooth connection between Urbach region α_U (as given by Eq. 1) and the intrinsic region α_I (as given by Eq.10), we require:

$$\begin{cases} \alpha_U\big|_{\hbar\omega=E_0} = \alpha_I\big|_{\hbar\omega=E_0} \\ \left.\dfrac{d(\alpha_U)}{d(\hbar\omega)}\right|_{\hbar\omega=E_0} = \left.\dfrac{d(\alpha_I)}{d(\hbar\omega)}\right|_{\hbar\omega=E_0} \end{cases} \tag{13}$$

Because the Urbach tail energy spans only a few meV, the corresponding k is very small. Using Eq. 4 to approximate E_c(k) and $E_{lh}(k)$, we obtain from Eq. 13 the condition:

$$E_0 \cong E_g + \frac{W}{2} \tag{14}$$

Recall that W is the Urbach tail energy. E_0 is the point where the absorption coefficient transitions from Urbach's rule to the intrinsic band-to-band behavior. E_0 was defined as the optical energy band

gap of HgCdTe by Chu *et al.*[28] The first derivative of the absorption coefficient peaks at E_0 since the rapid rise of the absorption coefficient following the exponential Urbach rule stops at this point[22,29]. Similar suggestions were made by Ariel et al.[30,31]

The combination of Eqs. 1, 10 and 14 gives the absorption coefficients near the band gap E_g as:[32]

$$\alpha(\hbar\omega)=\begin{cases}\dfrac{B}{E_g+\dfrac{W}{2}}\left[(\dfrac{W}{2}+b)\sqrt{(\dfrac{W}{2}+b)^2-b^2}+\dfrac{1}{8}(\dfrac{W}{2}+2b)\sqrt{(\dfrac{W}{2}+2b)^2-(2b)^2}\right]\cdot\exp\left(\dfrac{\hbar\omega}{W}\right) & (\hbar\omega\le E_g+W/2)\\ \dfrac{B}{\hbar\omega}\left[(\hbar\omega-E_g+b)\sqrt{(\hbar\omega-E_g+b)^2-b^2}+\dfrac{1}{8}(\hbar\omega-E_g+2b)\sqrt{(\hbar\omega-E_g+2b)^2-(2b)^2}\right] & (\hbar\omega\ge E_g+W/2)\end{cases} \quad (15)$$

here E_g is the band gap of HgCdTe, W is the Urbach tail energy in the same unit of E_g, parameters of b and B as functions of temperature and Cd composition in HgCdTe, can be determined by fitting experimental data. This formula is plotted in Fig. 3 for an x=0.21 $Hg_{1-x}Cd_xTe$ sample at 77 K and gives good agreement with experimental data both below and above E_0. In contrast, the parabolic model shows obvious deviations from experimental data at an energy of about 50 meV above E_g. Therefore, using parabolic model tends to predict a much smaller cut-off blue-shift with decreasing absorber layer thickness. To obtain the best fits, we fit not only the absorption coefficient but also the first order derivative of the absorption coefficient curve, as shown in Fig. 4.

If under certain circumstances W is so large as to be beyond the energy region in which the absorption coefficient is proportional to ε^{γ} ($0.5<\gamma\le 2$), then the following relationship can be obtained from Eq.13: $E_0 \cong E_g+\gamma\cdot W$.

Conclusions

An analytical model describing the absorption behavior of long wavelength infrared HgCdTe as a function of absorbed photon energy was established based on *k.p* electronic band structure

calculations. The model is capable of describing both the Urbach tail region and the intrinsic region up to at least 300 meV above the band gap. The intrinsic band-to-band absorption coefficient is proportional to $(\hbar\omega - E_g)^{\gamma}$ with γ increasing from 0.5 and 2 with increasing photon energy, a consequence of the nonparabolic conduction and light hole band dispersion relationships.

Acknowledgements

This work was partially supported by the DoD Multidisciplinary University Research Initiative (MURI) program monitored by Dr. W.W. Clark and administered by the Army Research Office under Grant number DAAD19-01-1-0462; partially supported by the Air Force Research Laboratory at Wright-Patterson AFB subcontracted through Anteon Corporation under contract number: USAF-5400-03-SC-0009; and partially supported by Air Force Office of Scientific Research under contract number: FA9550-06-C-0007 and monitored by Dr. D. J. Silversmith.

References:

(I will move them from the endnotes to here before submission)

Figure Captions:

Fig.1. Calculated 77 K 50% cut-off wavelengths and equivalent Cd compositions for $Hg_{1-x}Cd_xTe$ detectors with 10 μm thick absorber layers as a function of absorber layer thickness.

Fig.2. (a) Energy band structure of $Hg_{0.77}Cd_{0.23}Te$ near the Γ point at 300 K calculated using a 14×14 matrix k.p method, (b) 200 K, (c) 100 K and (d) 77 K. Solid line: conduction band; dashed line: heavy hole band; dash-dotted line: light hole; and dash-dot-dotted line: spin split-off band. (e) Open circles: calculated results from (d) for the conduction band; solid line: fitted Eq. 3 in text; dash-dot-dotted line (visible only near k=0): high energy asymptotes of hyperbola; and dashed line: fitted parabola, which deviates substantially from the other curves at higher energies. (f) Close-up of (e) near the bottom of the conduction band. Solid line: fitted using a hyperbola, which show reasonably good agreement even at the bottom of the conduction band; and dashed line: fitted using a parabola, which shows good agreement only very near the band gap. The dash-dot-dotted lines are asymptotes of the hyperbola.

Fig.3. Open squares: experimentally measured absorption coefficient of a $Hg_{0.79}Cd_{0.21}Te$ sample at 80 K; thin solid line: fitted Eq. 10 by assuming hyperbolic bands; dotted line: fitted Urbach tail (Eq.1) with $E_0=E_g+W/2$, here E_g is the theoretical band gap of HgCdTe, W is Urbach tail energy and E_0 is the optical band gap of HgCdTe as defined by the authors of Refs.11 and 24, which is the energy position of the peak in the first order deviative curve of the absorption coefficient as a function of absorbed photon energy; dashed line: fitted assuming parabolic bands, which shows reasonably good agreement only very near the band gap; and thick solid line: fitted using Eq.15. The insert is a close-up of the main figure and shows that Eq. 15 remains smooth at E_0.

Fig.4. Fitting of the fist derivative of the experimentally measured absorption coefficient shown in Fig.3 using the first derivative of Eq. 15 in the text.

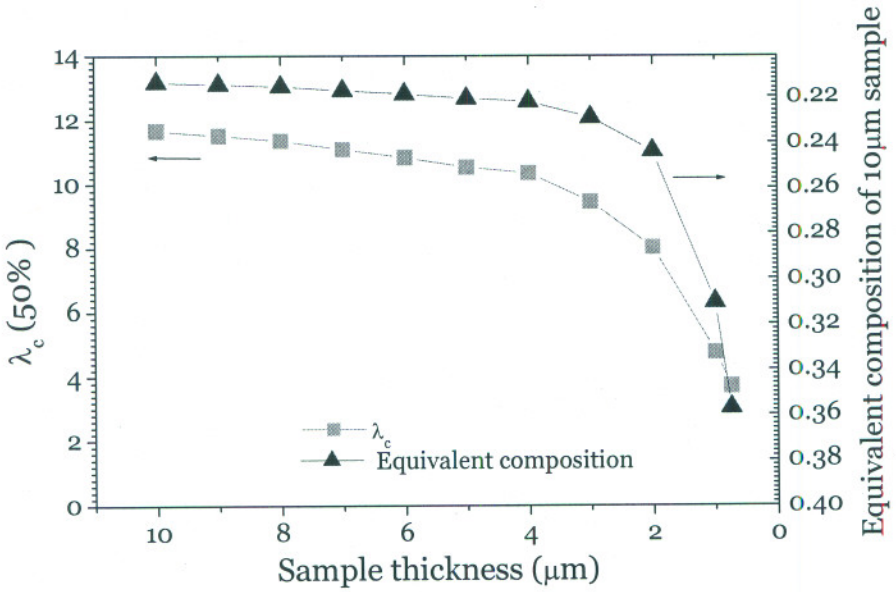
14
12
10
8
6
4
2
0
λ_c (50%)
0.22
0.24
0.26
0.28
0.30
0.32
0.34
0.36
0.38
0.40
Equivalent composition of 10μm sample
λ_c
Equivalent composition
10
8
6
4
2
0
Sample thickness (μm)

Figure 1

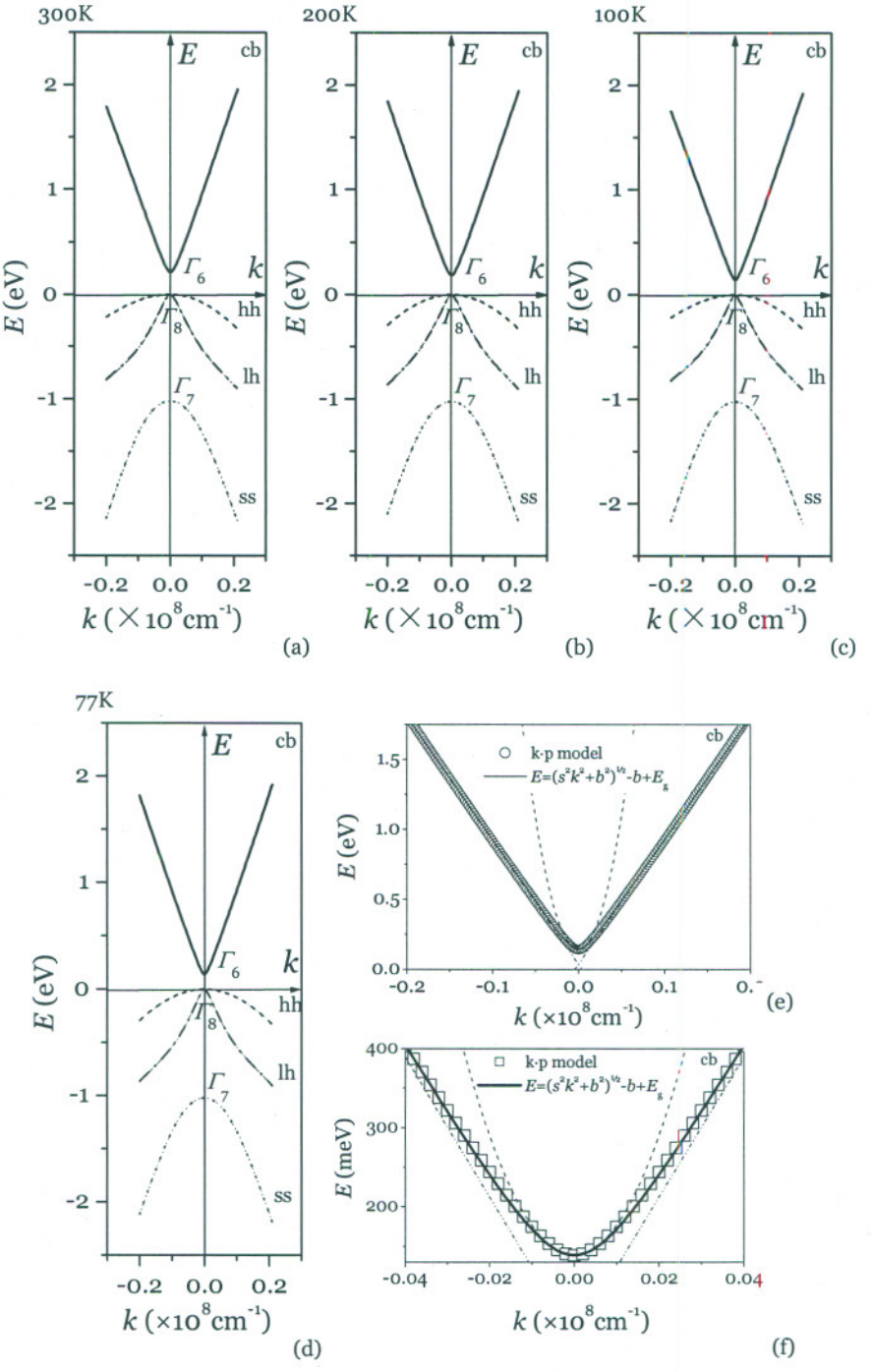
300K
200K
100K
77K
E
cb
k
Γ6
Γ8
Γ7
hh
lh
ss
E (eV)
k (×10^8 cm^-1)
(a)
(b)
(c)
(d)
k·p model
E=(s²k²+b²)^½-b+Eg
(e)
(f)
E (meV)

Figure 2

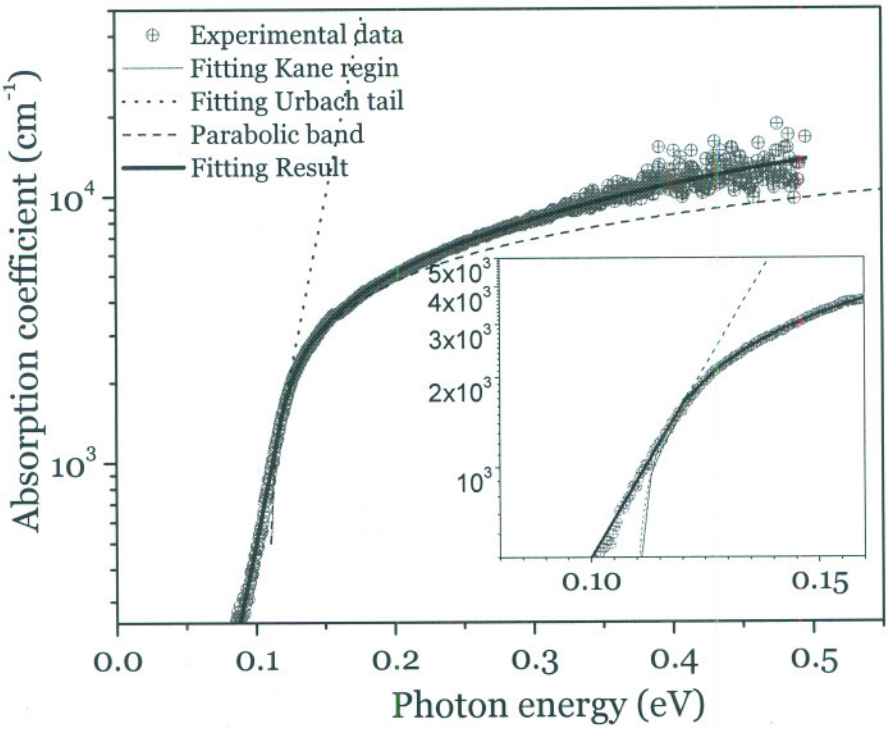
Experimental data
Fitting Kane regin
Fitting Urbach tail
Parabolic band
Fitting Result
Absorption coefficient (cm-1)
10^4
10^3
5x10^3
4x10^3
3x10^3
2x10^3
10^3
0.10
0.15
0.0
0.1
0.2
0.3
0.4
0.5
Photon energy (eV)

Figure 3

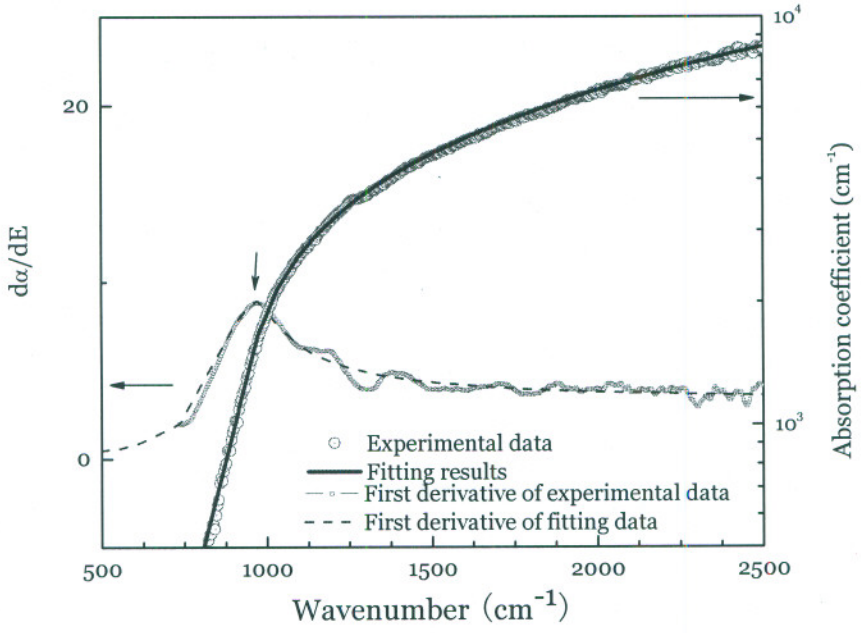
20
0
dα/dE
500
1000
1500
2000
2500
Wavenumber (cm-1)
10^4
10^3
Absorption coefficient (cm-1)
Experimental data
Fitting results
First derivative of experimental data
First derivative of fitting data

Figure 4

References:

[1] G. L. Hansen, J. L. Schmit and T. N. Casselman, J. Appl. Phys., 53, 7099(1982)

[2] M.W. Scott, J. Appl. Phys., 40, 4077(1969)

[3] E. Finkman and S.E. Schacham, J. Appl. Phys., 56, 2896(1984)

[4] Y. Chang, C. Fulk, J. Zhao, C.H. Grein and S. Sivananthan, Infrared Phys. Techn., in press

[5] L. A. Almeida, M. Thomas, W. Larsen, K. Spariosu, D. D. Edwall, J. D. Benson, W. Mason, A. J. Stoltz. and J. H. Dinan, J. Electron. Mater., 31, 669(2002)

[6] Y. Chang, G. Badano, E. Jiang, J.W. Garland, J. Zhao, C. H. Grein and S. Sivananthan, J. Cryst Growth., 277, 78(2005)

[7] Y. Chang, G. Badano, J. Zhao, C. H. Grein, S. Sivananthan, T. Aoki, and D. J. Smith, Appl. Phys. Lett., 83, 4785(2003)

[8] Y. Chang , J. Zhao, H. Abad, C. H. Grein, S. Sivananthan, T. Aoki and D. J. Smith, Appl. Phys. Lett., 86, 131924(2005)

[9] Y. Chang, C. H. Grein, J. Zhao, S. Sivanathan, C. Z. Wang, T. Aoki, D. J. Smith, P. S. Wijewarnasuriya and V. Nathan, J. Appl. Phys., accepted

[10] T. Aoki, D. J. Smith, Y. Chang, J. Zhao, G. Badano, C. Grein and S. Sivananthan, Appl. Phys. Lett., 82, 2275 (2003)

[11] T. Aoki, Y. Chang, G. Badano, J. Zhao, C. Grein, S. Sivananthan and D. J. Smith, J. Electron. Mater., 32(7), 703(2003)

[12] H.F. Schaake, J.H. Tregilgas, A.L. Lewis and P.M. Everett, J. Vac. Sci. Technol., A1, 1625(1983)

[13] see, for example, H. A. Macleod, Thin-film Optical Filters, American Elsevier Publishing Company, Inc., New York, 1969, Chapter 2

[14] D.D. Lofgreen, C.M. Peterson, A.A. Bell, M.F. Vilela and S.M. Johnson, J. Electrn. Mater., 35, 1487(2006)

[15] Y. Chang, G. Badano, J. Zhao, Y. D. Zhou, R. Ashokan, C. H. Grein and V. Nathan, J. Electron. Mater., 33, 709(2004)

[16] J. A. Mroczkowshi, D. A. Nelson, R. Murosako and P.H. Zimmermann, J. Vac. Sci. Tech., A1, 1758(1983)

[17] J. H. Chu, B. Li, K. Liu and D. Y. Tang, J. Appl. Phys., 75, 1234(1994)

[18] F. Urbach, Phys. Rev. 92, 1324(1953)

[19] C. H. Grein and S. John, Phys. Rev. B 39, 1140(1989)

[20] Y. Chang, C.H. Grein, S. Sivananthan, S. Guha, F. Aqariden and P. –K. Liao, Macroscopic and Microscopic Material Uniformity and Urbach Tail Energy Distribution of MBE-grown HgCdTe, The 24th (2005) US Workshop on the Physics and Chemistry of II-VI Materials, September 20-22, 2005, Boston, Massachusetts, USA.

[21] E. O. Kane, Phys. Chem. Solid., 1, 249(1957)

[22] J.H. Chu, Z.Y. Mi and D.Y. Tang, Infrared Phys. 32 195(1991)

[23] W. W. Anderson, Infrared Phys., 20, 363(1980)

[24] S. Krishnamurthy, A.-B. Chen and A. Sher, J. Appl. Phys., 80, 4045(1996)

[25] S.E. Schacham and E. Finkman, J. Appl. Phys., 57, 2001(1985)

[26] K. Moazzami, J. Phillips, D. Lee, S. Krishnamurthy, B. Benoit, F. Fink and T. Tiwald, J. Electron. Mater. 34, 773(2005)

[27] B. Li, Y.S. Gui, H. J. Ye, J.H.Chu and S. Krishnamurthy, J. Appl. Phys., 83, 7668(1998)

[28] J. H. Chu, S. Q. Xu and D. Y. Tang, Appl. Phys. Lett., 43, 1064(1983)

[29] B. Li, Y. Wu, Y. S. Gui, H. J. Ye, Y. Chang, L. He and J. H. Chu, Appl. Phys. Lett., 73, 1376(1998)

[30] V. Ariel, V. Garber, and G. Bahir, S. Krishnamurthy and A. Sher, Appl. Phys. Lett., 69, 1864(1996)

[31] V. Ariel, V. Garber, G. Bahir, A. Raizman and A. Sher, Appl. Phys. Lett., 70, 1849(1997)

[32] Y. Chang, C.H. Grein, S. Sivananthan, M.E. Flatte, V. Nathan and S. Guha, Appl. Phys. Lett., 89, 062109(2006)